Likert Scoring with Grade Decoupling for Long-term Action Assessment

Angchi Xu[1], Ling-An Zeng[2], Wei-Shi Zheng[1,3,4,*]
[1]School of Computer Science and Engineering, Sun Yat-sen University, China
[2]School of Artificial Intelligence, Sun Yat-sen University, China
[3]Peng Cheng Laboratory, Shenzhen, China
[4]Key Laboratory of Machine Intelligence and Advanced Computing, Ministry of Education, China
{xuangch, zenglan3}@mail2.sysu.edu.cn, wszheng@ieee.org

2022 IEEE/CVF Conference on Computer Vision and Pattern Recognition (CVPR) | 978-1-6654-6946-3/22/$31.00 ©2022 IEEE | DOI: 10.1109/CVPR52688.2022.00323

Abstract

Long-term action quality assessment is a task of evaluating how well an action is performed, namely, estimating a quality score from a long video. Intuitively, long-term actions generally involve parts exhibiting different levels of skill, and we call the levels of skill as performance grades. For example, technical highlights and faults may appear in the same long-term action. Hence, the final score should be determined by the comprehensive effect of different grades exhibited in the video. To explore this latent relationship, we design a novel Likert scoring paradigm inspired by the Likert scale in psychometrics, in which we quantify the grades explicitly and generate the final quality score by combining the quantitative values and the corresponding responses estimated from the video, instead of performing direct regression. Moreover, we extract grade-specific features, which will be used to estimate the responses of each grade, through a Transformer decoder architecture with diverse learnable queries. The whole model is named as Grade-decoupling Likert Transformer (GDLT), and we achieve state-of-the-art results on two long-term action assessment datasets.[1]

1. Introduction

Action quality assessment (AQA) is a task to evaluate how well a specific action is performed and is usually modeled as a score regression task. Due to its rich application scenarios in the real world, such as sport events [16, 27, 30–32, 37, 43–45], surgical training [10–12, 21, 41] and daily skills [8, 9, 18], AQA has attracted growing attention from the computer vision community.

Compared with actions that only take a few seconds (*e.g.*, diving), AQA of *long-term* actions (*e.g.*, figure skating) is more challenging since they contain richer and more complex information. Intuitively, **a long video is very likely to exhibit different levels of skill (*e.g.*, excellent, good, fair or poor) at different parts [9], and we call the levels of skill as performance *grades*.** For example, a perfect air twist, a substandard leg lifting, and a fall fault may occur in the same long-term action (figure skating). Therefore, we conceive that the quality score should be determined by the comprehensive effect of different grades exhibited in a video. In other words, we suppose that there exists an inherent mapping from grades to scores. This observation has hardly been discussed in pre-

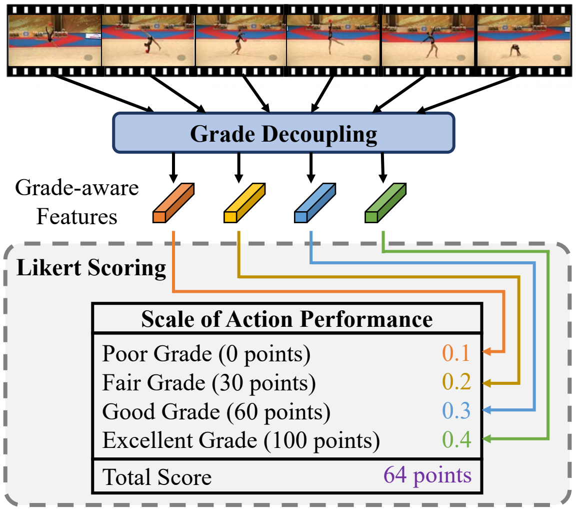
Grade Decoupling
Grade-aware Features
Likert Scoring
Scale of Action Performance
Poor Grade (0 points) 0.1
Fair Grade (30 points) 0.2
Good Grade (60 points) 0.3
Excellent Grade (100 points) 0.4
Total Score 64 points

Figure 1. A brief illustration of our idea. The features of an action video are first disentangled into different grade-aware features, which contain the information related to specific grades. Then they will be regarded as "evidence" to generate responses and "fill" the "scale". The final quality score is generated by aggregating the scores of "scale questions" (*i.e.*, different grades) according to the responses from the video.

[*] Corresponding author.

[1] Project page https://isee-ai.cn/~angchi/CVPR22_GDLT.html

978-1-6654-6946-3/22/$31.00 ©2022 IEEE
DOI 10.1109/CVPR52688.2022.00323

vious works [21, 27, 43, 45], and these existing works use MLP to directly regress the score from video representations, ignoring this inherent complexity.

In this work, we aim to explicitly model the influences of different grades on the score. To this end, we propose a novel scoring paradigm, named **Likert scoring**, which is inspired by the well-known *Likert scale* [19] in psychometrics and sociological investigation. A scale is a psychometric tool for quantitatively evaluating the psychological state of the respondent, which consists of several related questions or statements about different aspects. The respondent is asked to evaluate how well he/she agrees with each statement. Then the agreement degrees of each statement will be converted into quantified scores, and all scores are added to get a total score, which indicates the respondent's mentality. In the context of this paper, we treat assessing a complex action as filling a "scale", *whose "statements (questions)" refer to the inherent performance grades*. The input video is then required to "answer" the questions that *how well it matches each grade*, *i.e.*, the *response intensities* are estimated for each grade from the video. These intensities will be combined with the pre-quantified scores to determine the final quality score. The underlying insight here is to evaluate a complex objective (*i.e.*, action quality) by explicitly measuring several inherent components, which is consistent with the Likert scale. A brief illustration of this idea is shown in Figure 1.

Moreover, to fill the "scale", we need *"evidence"* for each question (*i.e.*, the information related to each grade from the video) to generate responses. For this purpose, we disentangle video features into different grade-aware features, which contain the grade-specific information. This procedure is called **grade decoupling**. Inspired by DETR [3], this step is implemented by a Transformer [39] decoder, which ingests a video feature sequence and a set of learnable vectors serving as the *prototypes* of various grades, and the grade-specific semantics are extracted from video features by these prototypes via the cross-attention mechanism.

Formally, we name our whole model as **Grade-decoupling Likert Transformer** (GDLT), which is composed of a standard Transformer [39] encoder-decoder architecture and a Likert Scoring Module (LSM). The former consists of a Temporal Context Encoder (TCE) and a Grade-aware Decoder (GAD). In the TCE, we leverage the self-attention mechanism to better explore the rich context information for each segment, which is critical for long video understanding. Then the GAD and LSM will perform grade decoupling and Likert scoring respectively. In summary, our main contributions are two-fold:

- A novel assessment paradigm named Likert scoring inspired by psychological research is proposed to explore the comprehensive effect of different grades on the score.
- A Transformer [39] encoder-decoder architecture is introduced to perform grade decoupling, which aims to extract grade-specific features used for Likert scoring from the input video. To the best of our knowledge, it is the first work to adopt the Transformer in AQA.

To evaluate our idea, we conduct experiments on two public long-term action assessment datasets: Rhythmic Gymnastics [45] and Fis-V [43]. Our model achieves state-of-the-art results on both datasets, demonstrating its effectiveness.

2. Related Work

Action Quality Assessment. AQA is generally regarded as a regression problem [11,16,21,27,28,30–32,40,43–45], *i.e.*, estimating a quality score for an action. Some early works [31, 32] directly adopt support vector regression to perform regression with the hand-crafted discrete cosine transform or deep C3D [38] features as input. To achieve a more accurate assessment, recent works [11, 16, 27, 28, 37, 40, 43–45] aim to solve some specific problems in AQA. For example, Tang *et al.* [37] utilize the label distribution learning to model score uncertainty. However, problems in *long-term* AQA are still relatively unexplored [43, 45]. Xu *et al.* [43] propose two LSTMs [14] to learn both local and global information. Zeng *et al.* [45] leverage static posture information to enhance video motion features and design a graph-based attention module for long-term temporal modeling. In this work, we explore various grades of performance implied in long videos and propose a novel scoring paradigm considering these grades instead of directly regressing the score.

However, Some daily activities such as tying a tie have no professional criteria for accurate scoring. Doughty *et al.* [8, 9] address this issue by regarding AQA as a pairwise ranking problem, *i.e.*, to determine which of a given pair of videos is better. Note that in [9], they propose separately modeling high-skill and low-skill parts in a video, and design loss functions to constrain the relationships between these two parts between a pair of videos, which is similar to our work. However, our proposed model is generalized to multiple grades instead of binary ones and can be used for direct score estimation.

Transformer. Transformer [39] was first introduced by Vaswani *et al.* for machine translation and sequence modeling. It proposes a self-attention mechanism allowing each element to see the whole sequence and to update itself by aggregating information from other elements. Due to its advanced ability to model global relationship, Transformer has dominated the natural language processing field [6, 33],

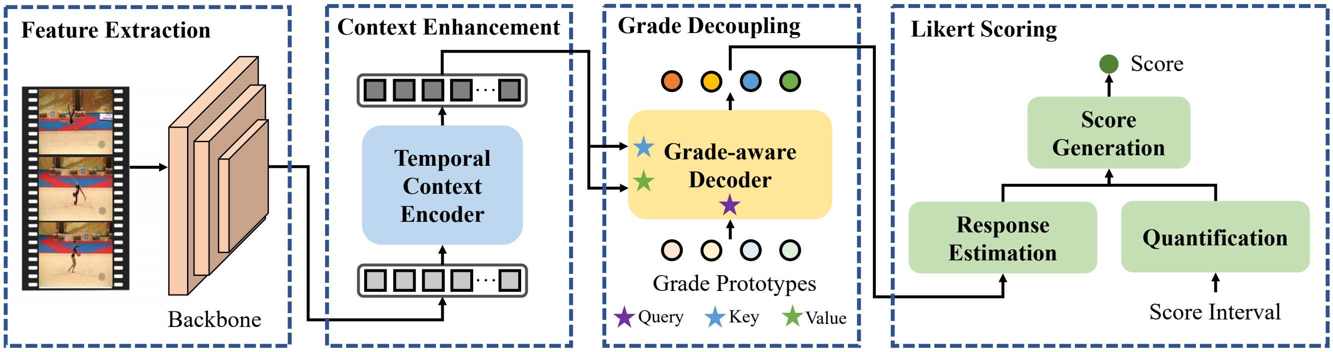

Figure 2. The overall framework of our proposed GDLT. The backbone extracts feature sequence from video segments, and the TCE enhances it by the context information. The GAD maintains a set of learnable vectors serving as prototypes of performance grades and exploits them to extract grade-aware features from context-enhanced video features. Finally, the grade-aware features are used to generate response intensities, which will be combined with quantitative values to calculate the final score.

as well as been widely adopted in time series modeling [42, 47] and computer vision tasks [1–3, 7, 22]. In this work, a transformer encoder is utilized to further explore the temporal context relationships in the video feature sequence.

Additionally, several works adopt a set of learnable queries with specific semantic meanings to extract diverse semantics from input via Transformer decoder [3, 17, 25, 36, 46]. For instance, DETR [3] uses each query to represent a potential object class in object detection. In this work, we regard the learnable queries as the prototypes of grades, which will be used to extract the relevant information for each grade via Transformer decoder.

3. Our Approach

In this section, we introduce our proposed Grade-decoupling Likert Transformer (GDLT) in detail. We first describe some preliminaries of our work in Section 3.1. Then we introduce three main components of GDLT, *i.e.*, Temporal Context Encoder (TCE), Grade-aware Decoder (GAD), and Likert Scoring Module (LSM) in Section 3.2, Section 3.3 and Section 3.4, respectively. Figure 2 illustrates the overall framework of the GDLT.

3.1. Preliminaries

Problem Formulation. We first formulate the AQA problem. Following the practice in the real world (*e.g.*, sports competitions), the action quality is measured by a score, which is a non-negative real number, and **a higher score indicates better action quality.** Naturally, the model is required to learn a mapping from videos to scores under the supervision of human expert annotations. Following [45], we normalize the labels to the interval [0,1] for more stable training.

Feature Extraction. Following the practice in long-term action understanding [15, 43, 45, 46, 48], we build GDLT upon the feature sequences extracted from non-overlapping video segments, each of which consists of several consecutive frames. The features are extracted via a well-designed video backbone (*e.g.*, I3D [5], TSM [20], and VST [23]). Then, a 2-layer MLP is applied for reducing the dimension of backbone features. We denote the obtained feature sequence of a video with T segments as $\{\boldsymbol{f}_t\}_{t=1}^{T}$ where $\boldsymbol{f}_t \in \mathbb{R}^d$, serving as the input for GDLT.

Grade Definition. As described in Section 1, the *grade* is the level of quality. In this work, we define K grades, indexed from 1 to K, to **indicate action quality from bad to good with ascending index**. Note that these grade indices are **consistent** with the subscripts of the grade prototypes (see Section 3.3), quantitative values (see Section 3.4) and other relevant symbols, namely, a relevant symbol with subscript k corresponds to the k-th grade.

3.2. Temporal Context Encoder

Since the features are independently extracted from the video segments, each $\boldsymbol{f}_t$ only contains information of a very small temporal region (*i.e.*, current segment) and lacks olinganxthe context information. Therefore, a Transformer [39] encoder is adopted to first enrich segment-wise representations $\{\boldsymbol{f}_t\}_{t=1}^{T}$. The context information of each segment is obtained through weighted aggregation among all segment features, and the weights are determined by the semantic correlations between the current segment and others. This procedure is called the *self-attention* mechanism. Then the context information is added back to the original $\boldsymbol{f}_t$, and the summed vectors are passed into a small feed-forward network for further fusion. Multiple encoders can be stacked to gradually aggregate and refine context semantics. We denote the final context-enhanced features as $\{\boldsymbol{f}_t^{ctx}\}_{t=1}^{T}$, which will be used by the Grade-aware Decoder.

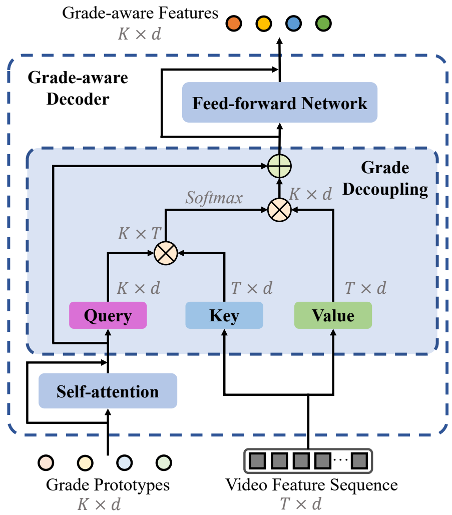

Figure 3. Illustration of the Grade-aware Decoder and grade decoupling mechanism. The shapes of important tensors are shown in gray. ⊗ denotes matrix multiplication. ⊕ denotes element-wise sum and is omitted in some residual connections for brevity. *Query*, *Key* and *Value* are three different linear projections.

3.3. Grade-aware Decoder

In the Grade-aware Decoder, we aim to extract the information related to different grades from context-enhanced video features $\{\boldsymbol{f}_t^{ctx}\}_{t=1}^{T}$. For this purpose, we introduce a set of K learnable vectors $\{\boldsymbol{p}_k\}_{k=1}^{K}$ as the *prototypes* of K performance grades to learn the distinct characteristics of them. Then inspired by DETR [3], the interaction between $\{\boldsymbol{p}_k\}_{k=1}^{K}$ and $\{\boldsymbol{f}_t^{ctx}\}_{t=1}^{T}$ is implemented by a *parallel non-autoregressive* and *non-masked* version of Transformer [39] decoder that consists of three parts: self-attention, cross-attention and a small feed-forward network (FFN). The self-attention mechanism is first applied for mining the relationships among K prototypes. We denote the updated prototypes after the self-attention as $\{\hat{\boldsymbol{p}}_k\}_{k=1}^{K}$. Then they will be used to extract the relevant information from video feature sequences through cross-attention, and this procedure is called grade decoupling. Figure 3 shows the details of GAD.

Grade Decoupling. The grade decoupling is implemented by the cross-attention mechanism. Specifically, the module takes $\{\boldsymbol{f}_t^{ctx}\}_{t=1}^{T}$ and $\{\hat{\boldsymbol{p}}_k\}_{k=1}^{K}$ as input, and first generates *queries* from $\{\hat{\boldsymbol{p}}_k\}_{k=1}^{K}$, while *keys* and *values* are transformed from $\{\boldsymbol{f}_t^{ctx}\}_{t=1}^{T}$ via three different linear projections:

$$\boldsymbol{q}_k = \boldsymbol{W}_q \hat{\boldsymbol{p}}_k,\ \boldsymbol{k}_t = \boldsymbol{W}_k \boldsymbol{f}_t^{ctx},\ \boldsymbol{v}_t = \boldsymbol{W}_v \boldsymbol{f}_t^{ctx}, \tag{1}$$

where $\{\boldsymbol{q}_k\}_{k=1}^{K}$, $\{\boldsymbol{k}_t\}_{t=1}^{T}$ and $\{\boldsymbol{v}_t\}_{t=1}^{T}$ indicate queries, keys and values, respectively. After that, the semantic correlation between k-th grade and t-th video segment is measured by dot-product similarity between corresponding query-key pair:

$$a_{k,t} = \frac{\boldsymbol{q}_k^T \boldsymbol{k}_t}{\sqrt{d}}, \tag{2}$$

where $\sqrt{d}$ serves as a scaling factor. It shows how much the t-th segment is related to the k-th performance grade. The softmax function is then applied along *temporal* dimension t to produce normalized *attention weights* $\hat{a}_{k,t}$ for information aggregation among values:

$$\boldsymbol{p}_k^{agg} = \sum_{t=1}^{T} \hat{a}_{k,t} \boldsymbol{v}_t. \tag{3}$$

The above equation is applied for pooling video features via *grade-dependent* weights. Therefore, the results can be regarded as a kind of "*pure substance*" containing information only related to specific grades in the video, ideally.

We then leverage the obtained $\{\boldsymbol{p}_k^{agg}\}_{k=1}^{K}$ to *activate* video-agnostic prototypes $\{\hat{\boldsymbol{p}}_k\}_{k=1}^{K}$ by adding $\{\boldsymbol{p}_k^{agg}\}_{k=1}^{K}$ back to $\{\hat{\boldsymbol{p}}_k\}_{k=1}^{K}$, and the summed vectors are further refined by the FFN. Multiple decoders can also be stacked and the output of one layer serves as the input *queries* for the next one. The output of the last GAD layer is denoted as $\{\boldsymbol{p}_k^{att}\}_{k=1}^{K}$, and we call it grade-aware features.

Diversity of the Grade-aware Features. Intuitively, different grade prototypes should focus on different semantic patterns, so the grade-aware features should have low correlation. Therefore, we exploit a *diversity loss* to regularize them explicitly, inspired by [17, 36]. Specifically, we adopt a triplet loss [34] to ensure that the grade-aware features of different grades are far enough apart. Given a batch of B videos, we rewrite $\{\boldsymbol{p}_k^{att}\}_{k=1}^{K}$ as $\{\boldsymbol{p}_k^{att,(i)}\}_{k=1}^{K}$ where $i = 1, 2, ..., B$. Each triplet consists of a grade-aware feature $\boldsymbol{p}_k^{att,(i)}$ of the k-th grade and i-th video as an anchor, a positive sample with the same grade and a negative one with a different grade. Hence, for each $\boldsymbol{p}_k^{att,(i)}$, we search for the *hardest positive* and *negative* pair distances $D_+^{i,k}$ and $D_-^{i,k}$ with:

$$\begin{aligned} D_+^{i,k} &= \max_j dist(\boldsymbol{p}_k^{att,(i)}, \boldsymbol{p}_k^{att,(j)}),\ j \neq i, \\ D_-^{i,k} &= \min_{m,n} dist(\boldsymbol{p}_k^{att,(i)}, \boldsymbol{p}_m^{att,(n)}),\ m \neq k, \end{aligned} \tag{4}$$

where $dist(\cdot,\cdot)$ is a pairwise distance metric. We use the cosine distance here:

$$dist(\boldsymbol{x}, \boldsymbol{y}) = 1 - \frac{\langle \boldsymbol{x}, \boldsymbol{y} \rangle}{\|\boldsymbol{x}\|_2 \|\boldsymbol{y}\|_2}. \tag{5}$$

Then the diversity loss is defined as:

$$\mathcal{L}_{div} = \frac{1}{BK} \sum_{i=1}^{B} \sum_{k=1}^{K} max(0, D_+^{i,k} - D_-^{i,k} + \alpha), \tag{6}$$

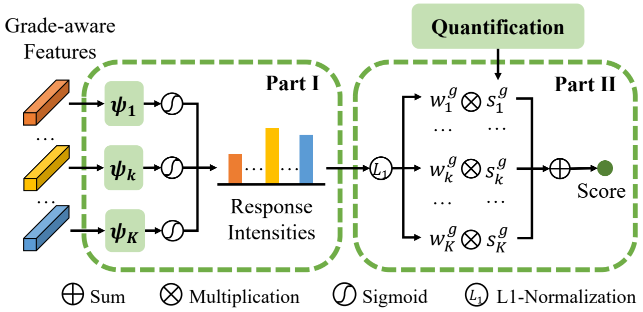

Figure 4. Illustration of Likert Scoring Module. **Part I:** response estimation. **Part II:** score generation.

where α is a non-negative margin and a hyper-parameter.

3.4. Likert Scoring Module

For bridging grades and the quality score, we design this Likert Scoring Module inspired by the Likert scale [19], in which we apply discrete values for quantifying each grade and generate a quality score by combining them. The combination weights are considered as the *response intensities* of each grade in the video and are estimated from the grade-aware features $\{\boldsymbol{p}_k^{att}\}_{k=1}^K$, since each of them can be regarded as a global representation of a specific performance grade in the video. Formally, the Likert scoring paradigm is composed of three steps: quantification, response estimation, and score generation. A brief illustration is given in Figure 4.

Quantification. The first step is to find a set of discrete values $\{s_k^g\}_{k=1}^K$ to represent grade, which are fixed for a given dataset. Obviously, these values should cover the whole valid score interval [0,1], and be diverse enough to ensure the discriminability of grades. Hence, we set them uniformly distributed in the interval:

$$s_k^g = \frac{k-1}{K-1}. \tag{7}$$

We also examine other choices in ablation studies.

Response Estimation. After GAD, the grade-aware feature $\boldsymbol{p}_k^{att}$ should contain information related to the k-th performance grade in the video. Therefore, we adopt a simple network $\psi_k(\cdot)$ to estimate the response intensity to the k-th grade (denoted as $\hat{w}_k^g$) of the video from the corresponding feature $\boldsymbol{p}_k^{att}$. $\psi_k(\cdot)$ is implemented as a full-connected layer, followed by a sigmoid activation σ:

$$\hat{w}_k^g = \sigma(\psi_k(\boldsymbol{p}_k^{att})). \tag{8}$$

Note that for learning the specific mapping rules for different grades, the parameters among $\psi_k(\cdot)$ are not shared.

Score Generation. The final score is generated through a linear combination of quantitative values and response intensities among grades. Note that the score should be determined by the *proportion* of each grade to ensure that it falls within a valid interval (*i.e.*, [0,1]). Hence we normalize $\{\hat{w}_k^g\}_{k=1}^K$ such that the sum is 1 to obtain new weights $\{w_k^g\}_{k=1}^K$:

$$w_k^g = \frac{\hat{w}_k^g}{\sum_{i=1}^K \hat{w}_i^g}. \tag{9}$$

Finally, the quality score s is calculated as:

$$s = \sum_{k=1}^K w_k^g s_k^g. \tag{10}$$

Loss Function. To directly minimize the errors between estimated scores and labels, we adopt the mean-squared error (MSE) loss $\mathcal{L}_{MSE}$ to train our model, together with the diversity loss term $\mathcal{L}_{div}$ described in Section 3.3:

$$\mathcal{L} = \mathcal{L}_{MSE} + \lambda \mathcal{L}_{div}, \tag{11}$$

where λ is a trade-off hyper-parameter.

4. Experiments

We conduct experiments on two datasets: Rhythmic Gymnastics [45] and Fis-V [43] to evaluate our model. We first briefly introduce the datasets and common metric. Then, we describe our implementation details and present the results. After that, we perform ablation studies to further analyze our model in depth and conduct some visualization for intuitive understanding.

4.1. Datasets and Metric

Rhythmic Gymnastics (RG). The RG dataset contains a total of 1000 videos of 4 rhythmic gymnastics actions with different apparatuses, *i.e.*, ball, clubs, hoop, and ribbon. The length of each video is approximately 1.6 minutes with a frame rate of 25. There are 200 videos for training and 50 for evaluating in each kind of action. Following the practice of [45], we train individual models for each kind.

Figure Skating Video (Fis-V). The Fis-V dataset has 500 videos of ladies' singles short program of figure skating. Each video is approximately 2.9 minutes long with a frame rate of 25. We follow the official split which has 400 videos for training and 100 for testing. All videos are annotated with two scores, namely, *Total Element Score* (TES) and *Total Program Component Score* (PCS), according to the competition rule. Following [43], we train two independent models for predicting these two scores.

Note that Fis-V is a substitute for MIT-Skating [32] and UNLV-Skating [31] , which are also about figure skating but much smaller (150/171 videos, respectively). Thus, we no longer conduct experiments on them.

Methods	Features	SRCC↑							
		Rhythmic Gymnastics					Fis-V		
		Ball	Clubs	Hoop	Ribbon	Avg.	TES	PCS	Avg.
C3D+SVR [31]	C3D [38]	0.357 [45]	0.551 [45]	0.495 [45]	0.516 [45]	0.483 [45]	0.400 [43]	0.590 [43]	0.501 [43]
MS-LSTM [43]	C3D [38]	-	-	-	-	-	0.650	0.780	0.721
	I3D [5]	0.515 [45]	0.621 [45]	0.540 [45]	0.522 [45]	0.551 [45]	-	-	-
	VST [23]	0.621†	0.661†	0.670†	0.695†	0.663†	0.660†	$\underline{0.809}$†	0.744†
ACTION-NET [45]	I3D [5] + ResNet [13]	0.528	0.652	0.708	0.578	0.623	-	-	-
	VST [23] + ResNet [13]	$\underline{0.684}$†	$\underline{0.737}$†	$\underline{0.733}$†	**0.754**†	$\underline{0.728}$†	**0.694**†	$\underline{0.809}$†	$\underline{0.757}$†
GDLT (Ours)	VST [23]	**0.746**	**0.802**	**0.765**	$\underline{0.741}$	**0.765**	$\underline{0.685}$	**0.820**	**0.761**

Table 1. Comparisons of GDLT with other methods on RG and Fis-V datasets. Avg. is the average SRCC across all classes computed using Fisher's z-value. † indicates the results of our reimplementation. ↑ indicates that the higher the metric, the better. Best results are in bold, second best are underlined.

Metric. Following previous works [31, 32, 43, 45], we adopt the Spearman's rank correlation coefficient (SRCC) ρ as the evaluation metric, which measures the monotonicity between the predicted series and the ground-truth series. It's defined as follows:

$$\rho = \frac{\sum_i (x_i^r - \bar{x}^r)(y_i^r - \bar{y}^r)}{\sqrt{\sum_i (x_i^r - \bar{x}^r)^2 \sum_i (y_i^r - \bar{y}^r)^2}}, \tag{12}$$

where x^r and y^r indicate the *rankings* of two series respectively. It ranges from -1 to 1 and the higher is the better. In addition, the average SRCC across classes (the word "class" refers to both *action types* in RG and *score types* in Fis-V) is calculated from individual per-class SRCCs using Fisher's z-value as in [11, 27, 29, 37, 44].

4.2. Implementation Details

Feature Extraction. As described in Section 3.1, we first divide the video into non-overlapping segments, each of which is composed of 32 consecutive frames. Due to the rapid development of vision Transformer in recent years, we adopt a newly developed Video Swin Transformer (VST) [23] pretrained on Kinetics-600 [4], which is extended from Swin Transformer [22], as our backbone. Note that we don't fine-tune it, following previous works on long-term action understanding [15, 43, 45, 48]. For mini-batch training, the number of segments is fixed to 68 for RG and 124 for Fis-V. If a video has more segments, we select continuous segments where the start position is randomly determined in each training iteration, as in [43, 45]. All segments are used when testing.

Experimental Settings. We use the 1-layer TCE and 2-layer GAD all with single-head attention to implement GDLT. The dimension of the latent space d is 256, and the number of grades K is set as 4 for all classes. We use the SGD with a momentum of 0.9 to optimize all models. The batch size is 32 and the learning rate is 0.01, and we then gradually decrease it to 0.0001 by a cosine annealing strategy [24]. For better convergence, we set different epochs for different models: 250/400/500/150/320/400 for RG(Ball) / RG(Clubs) / RG(Hoop) / RG(Ribbon) / Fis-V(TES) / Fis-V(PCS). The λ in Equation (11) is 1.0 for RG and 0.5 for Fis-V. The α in Equation (6) is 1.0 for all models. To regularize the models, we use a dropout of 0.3/0.7 for RG/Fis-V and the weight decay is set as 1e-4. See more details in the supplementary material.

4.3. Comparison with the State-of-the-art

Table 1 shows the assessment results of our model and previous state-of-the-art methods on RG and Fis-V datasets. For fair comparison, we reimplement [43, 45] on the same VST features as ours. As shown in Table 1, our model outperforms the current state-of-the-art method ACTION-NET [45], especially on RG (by 0.037 on average), and achieves average improvements of 0.102 on RG and 0.017 on Fis-V compared with MS-LSTM [43]. Note that they both directly regress the score from the global feature of a video, so the results demonstrate the effectiveness of modeling the latent grades. Remarkably, ACTION-NET utilizes additional *static* image features to assist the dynamic video features. Instead, our GDLT uses video features only but still achieves superior results.

4.4. Ablation Studies

Likert Scoring Paradigm. To evaluate our proposed Likert scoring (LS) paradigm, we compare it with the common practice of AQA that directly regresses the score from the video-level global description via MLP. Hence, we adopt the common **average pooling (AVG)** and **attention pooling (ATT)** to generate this global description from the context-enhanced features $\{\boldsymbol{f}_t^{ctx}\}_{t=1}^T$, as two baselines. The attention unit consists of two fully-connected layers with ReLU and softmax activation functions [9, 26, 35, 45]. At each time step t, it takes the feature $\boldsymbol{f}_t^{ctx}$ as input and outputs a weight for aggregation.

Additionally, the output of Transformer [39] decoder (*i.e.*, GAD) can be seen as a set of *response features* corresponding to specific semantic patterns [3, 17, 25, 36, 46]. Therefore, to further show that the superiority is achieved

Encoder	Decoder	Rhythmic Gymnastics					Fis-V		
		Ball	Clubs	Hoop	Ribbon	Avg.	TES	PCS	Avg.
TCE	AVG	**0.773**	0.754	0.675	0.711	0.730	0.553	0.786	0.687
	ATT	0.711	0.685	0.696	0.728	0.705	0.528	0.776	0.670
	TD-IS	0.715	0.701	0.727	**0.755**	0.725	0.607	0.807	0.722
	TD-CS	0.697	0.719	0.736	0.696	0.712	0.573	**0.822**	0.720
	TD-AS	0.705	0.787	0.688	0.707	0.724	0.575	0.815	0.715
	TD-LS	0.746	**0.802**	**0.765**	0.741	**0.765**	**0.685**	0.820	**0.761**

Table 2. Ablation studies on the Likert scoring paradigm. AVG, ATT, TD-IS, TD-CS, TD-AS, and TD-LS indicate average pooling, attention pooling, Individual-Scoring, Concatenating-and-Scoring, Averaging-and-Scoring, and our Likert-Scoring, respectively. Best results are in bold, second best are underlined.

Variants	Rhythmic Gymnastics					Fis-V		
	Ball	Clubs	Hoop	Ribbon	Avg.	TES	PCS	Avg.
GDLT w/o TCE	0.725	0.693	0.669	**0.764**	0.715	0.597	0.777	0.698
GDLT w/o $\mathcal{L}_{div}$	0.723	0.755	0.760	0.700	0.735	0.675	0.816	0.754
GDLT	**0.746**	**0.802**	**0.765**	0.741	**0.765**	**0.685**	**0.820**	**0.761**

Table 3. Ablation studies on the impact of TCE and $\mathcal{L}_{div}$.

exactly by the scoring paradigm instead of the Transformer decoder, we construct three additional baselines (prefixed by "TD") that generate scores from these response features by some common manners:

- **Individual-Scoring (TD-IS).** This baseline individually regresses scores from each response feature through different MLPs and then averages them.
- **Concatenating-and-Scoring (TD-CS).** This baseline concatenates all response features as the global representation and regresses the score from it directly.
- **Averaging-and-Scoring (TD-AS).** This baseline is similar to TD-CS but TD-AS generates the global representation by averaging all response features.

The results are shown in Table 2. Our proposed Likert scoring achieves best or second-best performance on all classes and outperforms others with a large margin on average, showing its robustness and effectiveness. Especially, compared with TD-IS, TD-CS, and TD-AS, the results show that we establish a more direct and meaningful connection between the response features and the final score than them, as explained in Section 1.

Moreover, similar to [9], we have an interesting finding that the inclusion of the attention unit decreases the performance from naive average pooling in some cases. We think it's due to the huge gap between key segment selection and score regression. On the contrary, our model explicitly links the pooled features to specific grades. This operation can be regarded as an intermediate *bridge*, which alleviates the above gap and leads to superior results.

Impact of TCE. From Table 3, we can observe significant performance drops on both RG (-0.05) and Fis-V (-0.063) when removing the TCE from the full model. It demonstrates that the context information is important for long-term video understanding.

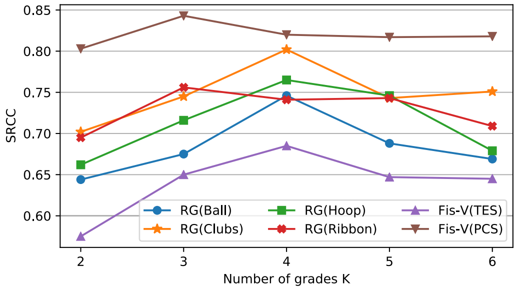

Figure 5. Comparison with different numbers of grades. Best viewed in color.

Impact of $\mathcal{L}_{div}$. As shown in Table 3, performance declines when $\mathcal{L}_{div}$ is not applied. $\mathcal{L}_{div}$ provides additional regularization to assist the learning of GAD, which lacks of any direct supervision signal (only video-level score labels are provided).

The Number of Grades K. The number of grades K is critical. As shown in Figure 5, $K = 4$ is suitable for all classes. We observe that the performance drops on most classes when increasing K, because too many grades may bring ambiguity to the model. Remarkably, the performance at $K = 2$ is relatively poor, which shows that the good/bad binary modeling [9] isn't enough for complex action.

Quantitative Strategies. In Equation (7), we uniformly set the quantitative values $\{s^g_k\}^K_{k=1}$. We call this method as *Uniform-Interval* (UI), and examine two other possible methods here (note that for covering the entire score interval [0,1], s^g_1 and s^g_K must be 0 and 1):

- **Uniform-Sample (US).** We quantify the grades so that the ground-truth scores of samples in training set are uniformly distributed in $K - 1$ intervals.
- **Learnable-Width (LW).** We make the quantitative values learnable by taking the widths of $K - 1$ intervals as a part of trainable parameters. When scoring, we apply the softmax function for making them non-negative and sum up to 1, and generate quantitative values by normalized widths.

As shown in Table 4, the simplest method UI achieves the best average performance. Remarkably, making quantitative values learnable doesn't improve the model since it may be difficult to optimize the model when both the values and combination weights are constantly changing.

4.5. Qualitative Analyses

Visualization of Cross-attention Weights. To figure out the patterns on which grade prototypes focus, we show

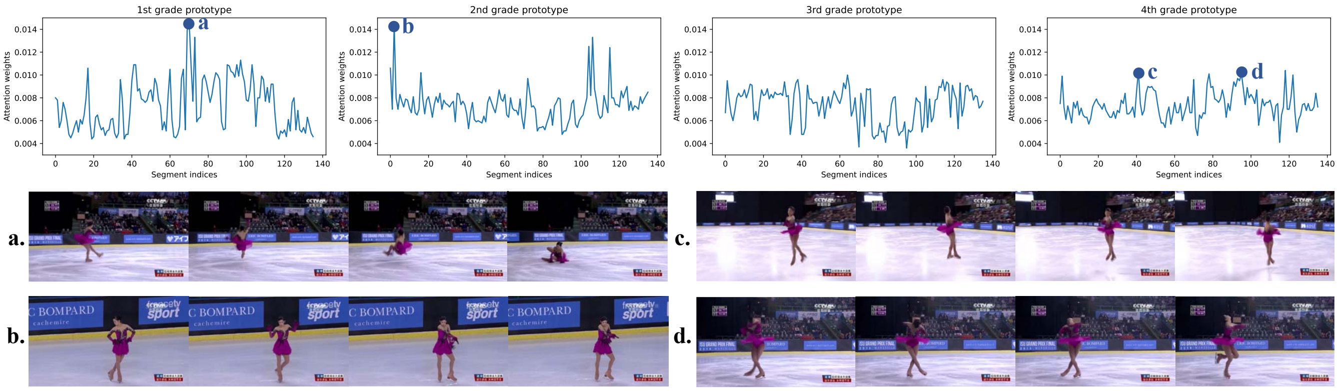

Figure 6. Visualization of cross-attention weights of each grade prototype in the last GAD layer. The sample is the *#17* video in Fis-V and the class is PCS. The first row shows four weight curves of four prototypes on video segments. The next two rows are four video segments corresponding to four markers on the curves, *i.e*., a, b, c, and d.

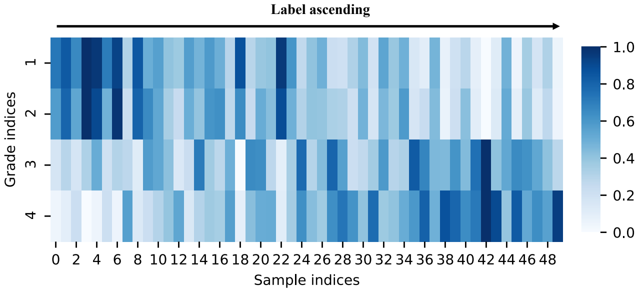

Figure 7. Visualization of response intensities at each grade of all video samples on the test set of RG(Ball). Each column represents a sample, and all samples are sorted in ascending order of label scores. To better observe the *relative* changes of intensities with the sample scores, we normalize each row, *i.e*., all intensities of the same grade, by min-max scaling. Best viewed in color.

Variants	Rhythmic Gymnastics					Fis-V		
	Ball	Clubs	Hoop	Ribbon	Avg.	TES	PCS	Avg.
US	**0.758**	0.775	0.741	**0.741**	0.754	0.652	0.799	0.734
LW	0.689	0.749	0.707	0.724	0.718	0.651	**0.820**	0.747
UI (Ours)	0.746	**0.802**	**0.765**	**0.741**	**0.765**	**0.685**	**0.820**	**0.761**

Table 4. Comparison with different strategies to quantify grades. US, LW, and UI indicate Uniform-Sample, Learnable-Width, and Uniform-Interval, respectively. Best results are in bold, second best are underlined.

in Figure 6 the cross-attention weights computed by Equation (2) of each prototype on a video feature sequence in the last GAD layer. The different fluctuations of weight curves demonstrate different attention patterns. Specifically, the 1st grade prototype gives high weight to the moment when an athlete falls (marker a), which indicates poor performance. The 2nd-grade prototype detects more trivial parts that cannot be given high scores (marker b). The curve of the 3rd grade is relatively stable since its quantitative value s_3^g (0.667) is closest to the average label score of the dataset, so its grade pattern might be common. Finally, some technical movements related to high skill are attended by the prototype of the highest grade, such as air twist (marker c) and spinning (marker d).

Visualization of Response Intensities. Figure 7 shows how the *response intensities* $\{\hat{w}_k^g\}_{k=1}^K$ estimated by Equation (8) of a trained model change with the label scores. We find that the intensity of low grades decreases almost monotonically with the increment of sample scores, while the intensity of high grades increases, which is in line with human experience. See more visualizations in the supplementary material.

5. Conclusion

In this work, we propose a novel Grade-decoupling Likert Transformer (GDLT) to explore the comprehensive effect of different grades exhibited in the video on the score. For this purpose, a new scoring paradigm named Likert scoring is proposed, in which we regard the quality score as the combination between quantified grades and corresponding responses estimated from the video. Besides, a Transformer decoder is adopted to extract the grade-specific information, which will be used for response estimation, from the video via diverse learnable queries. The state-of-the-art results on two long-term AQA datasets demonstrate the effectiveness of our model.

6. Acknowledgment

This work was supported partially by the NSFC (U21A20471, U1911401, U1811461), Guangdong NSF Project (No. 2020B1515120085, 2018B030312002), Guangzhou Research Project (201902010037), and the Key-Area Research and Development Program of Guangzhou (202007030004).

References

[1] Anurag Arnab, Mostafa Dehghani, Georg Heigold, Chen Sun, Mario Lučić, and Cordelia Schmid. Vivit: A video vision transformer. *arXiv preprint arXiv:2103.15691*, 2021. 3

[2] Gedas Bertasius, Heng Wang, and Lorenzo Torresani. Is space-time attention all you need for video understanding? *arXiv preprint arXiv:2102.05095*, 2021. 3

[3] Nicolas Carion, Francisco Massa, Gabriel Synnaeve, Nicolas Usunier, Alexander Kirillov, and Sergey Zagoruyko. End-to-end object detection with transformers. In *European Conference on Computer Vision*, pages 213–229. Springer, 2020. 2, 3, 4, 6

[4] Joao Carreira, Eric Noland, Andras Banki-Horvath, Chloe Hillier, and Andrew Zisserman. A short note about kinetics-600. *arXiv preprint arXiv:1808.01340*, 2018. 6

[5] Joao Carreira and Andrew Zisserman. Quo vadis, action recognition? a new model and the kinetics dataset. In *proceedings of the IEEE Conference on Computer Vision and Pattern Recognition*, pages 6299–6308, 2017. 3, 6

[6] Jacob Devlin, Ming-Wei Chang, Kenton Lee, and Kristina Toutanova. Bert: Pre-training of deep bidirectional transformers for language understanding. *arXiv preprint arXiv:1810.04805*, 2018. 2

[7] Alexey Dosovitskiy, Lucas Beyer, Alexander Kolesnikov, Dirk Weissenborn, Xiaohua Zhai, Thomas Unterthiner, Mostafa Dehghani, Matthias Minderer, Georg Heigold, Sylvain Gelly, et al. An image is worth 16x16 words: Transformers for image recognition at scale. *arXiv preprint arXiv:2010.11929*, 2020. 3

[8] Hazel Doughty, Dima Damen, and Walterio Mayol-Cuevas. Who's better? who's best? pairwise deep ranking for skill determination. In *Proceedings of the IEEE Conference on Computer Vision and Pattern Recognition*, pages 6057–6066, 2018. 1, 2

[9] Hazel Doughty, Walterio Mayol-Cuevas, and Dima Damen. The pros and cons: Rank-aware temporal attention for skill determination in long videos. In *Proceedings of the IEEE/CVF Conference on Computer Vision and Pattern Recognition*, pages 7862–7871, 2019. 1, 2, 6, 7

[10] Isabel Funke, Sören Torge Mees, Jürgen Weitz, and Stefanie Speidel. Video-based surgical skill assessment using 3d convolutional neural networks. *International journal of computer assisted radiology and surgery*, 14(7):1217–1225, 2019. 1

[11] Jibin Gao, Wei-Shi Zheng, Jia-Hui Pan, Chengying Gao, Yaowei Wang, Wei Zeng, and Jianhuang Lai. An asymmetric modeling for action assessment. In *European Conference on Computer Vision*, pages 222–238. Springer, 2020. 1, 2, 6

[12] Yixin Gao, S Swaroop Vedula, Carol E Reiley, Narges Ahmidi, Balakrishnan Varadarajan, Henry C Lin, Lingling Tao, Luca Zappella, Benjamın Béjar, David D Yuh, et al. Jhu-isi gesture and skill assessment working set (jigsaws): A surgical activity dataset for human motion modeling. In *MICCAI workshop: M2cai*, volume 3, page 3, 2014. 1

[13] Kaiming He, Xiangyu Zhang, Shaoqing Ren, and Jian Sun. Deep residual learning for image recognition. In *Proceedings of the IEEE conference on computer vision and pattern recognition*, pages 770–778, 2016. 6

[14] Sepp Hochreiter and Jürgen Schmidhuber. Long short-term memory. *Neural computation*, 9(8):1735–1780, 1997. 2

[15] Fa-Ting Hong, Jia-Chang Feng, Dan Xu, Ying Shan, and Wei-Shi Zheng. Cross-modal consensus network for weakly supervised temporal action localization. *arXiv preprint arXiv:2107.12589*, 2021. 3, 6

[16] Hiteshi Jain, Gaurav Harit, and Avinash Sharma. Action quality assessment using siamese network-based deep metric learning. *IEEE Transactions on Circuits and Systems for Video Technology*, 31(6):2260–2273, 2020. 1, 2

[17] Yulin Li, Jianfeng He, Tianzhu Zhang, Xiang Liu, Yongdong Zhang, and Feng Wu. Diverse part discovery: Occluded person re-identification with part-aware transformer. In *Proceedings of the IEEE/CVF Conference on Computer Vision and Pattern Recognition*, pages 2898–2907, 2021. 3, 4, 6

[18] Zhenqiang Li, Yifei Huang, Minjie Cai, and Yoichi Sato. Manipulation-skill assessment from videos with spatial attention network. In *Proceedings of the IEEE/CVF International Conference on Computer Vision Workshops*, pages 0–0, 2019. 1

[19] Rensis Likert. A technique for the measurement of attitudes. *Archives of psychology*, 1932. 2, 5

[20] Ji Lin, Chuang Gan, and Song Han. Tsm: Temporal shift module for efficient video understanding. In *Proceedings of the IEEE/CVF International Conference on Computer Vision*, pages 7083–7093, 2019. 3

[21] Daochang Liu, Qiyue Li, Tingting Jiang, Yizhou Wang, Rulin Miao, Fei Shan, and Ziyu Li. Towards unified surgical skill assessment. In *Proceedings of the IEEE/CVF Conference on Computer Vision and Pattern Recognition*, pages 9522–9531, 2021. 1, 2

[22] Ze Liu, Yutong Lin, Yue Cao, Han Hu, Yixuan Wei, Zheng Zhang, Stephen Lin, and Baining Guo. Swin transformer: Hierarchical vision transformer using shifted windows. *arXiv preprint arXiv:2103.14030*, 2021. 3, 6

[23] Ze Liu, Jia Ning, Yue Cao, Yixuan Wei, Zheng Zhang, Stephen Lin, and Han Hu. Video swin transformer. *arXiv preprint arXiv:2106.13230*, 2021. 3, 6

[24] Ilya Loshchilov and Frank Hutter. Sgdr: Stochastic gradient descent with warm restarts. *arXiv preprint arXiv:1608.03983*, 2016. 6

[25] Megha Nawhal and Greg Mori. Activity graph transformer for temporal action localization. *arXiv preprint arXiv:2101.08540*, 2021. 3, 6

[26] Phuc Xuan Nguyen, Deva Ramanan, and Charless C Fowlkes. Weakly-supervised action localization with background modeling. In *Proceedings of the IEEE/CVF International Conference on Computer Vision*, pages 5502–5511, 2019. 6

[27] Jia-Hui Pan, Jibin Gao, and Wei-Shi Zheng. Action assessment by joint relation graphs. In *Proceedings of the IEEE/CVF International Conference on Computer Vision*, pages 6331–6340, 2019. 1, 2, 6

[28] Jia-Hui Pan, Jibin Gao, and Wei-Shi Zheng. Adaptive action assessment. *IEEE Transactions on Pattern Analysis & Machine Intelligence*, 2021. 2

[29] Paritosh Parmar and Brendan Morris. Action quality assessment across multiple actions. In *2019 IEEE winter conference on applications of computer vision (WACV)*, pages 1468–1476. IEEE, 2019. 6

[30] Paritosh Parmar and Brendan Tran Morris. What and how well you performed? a multitask learning approach to action quality assessment. In *Proceedings of the IEEE/CVF Conference on Computer Vision and Pattern Recognition*, pages 304–313, 2019. 1, 2

[31] Paritosh Parmar and Brendan Tran Morris. Learning to score olympic events. In *Proceedings of the IEEE Conference on Computer Vision and Pattern Recognition Workshops*, pages 20–28, 2017. 1, 2, 5, 6

[32] Hamed Pirsiavash, Carl Vondrick, and Antonio Torralba. Assessing the quality of actions. In *European Conference on Computer Vision*, pages 556–571. Springer, 2014. 1, 2, 5, 6

[33] Alec Radford, Jeffrey Wu, Rewon Child, David Luan, Dario Amodei, Ilya Sutskever, et al. Language models are unsupervised multitask learners. *OpenAI blog*, 1(8):9, 2019. 2

[34] Florian Schroff, Dmitry Kalenichenko, and James Philbin. Facenet: A unified embedding for face recognition and clustering. In *Proceedings of the IEEE conference on computer vision and pattern recognition*, pages 815–823, 2015. 4

[35] Baifeng Shi, Qi Dai, Yadong Mu, and Jingdong Wang. Weakly-supervised action localization by generative attention modeling. In *Proceedings of the IEEE/CVF Conference on Computer Vision and Pattern Recognition*, pages 1009–1019, 2020. 6

[36] Rui Sun, Yihao Li, Tianzhu Zhang, Zhendong Mao, Feng Wu, and Yongdong Zhang. Lesion-aware transformers for diabetic retinopathy grading. In *Proceedings of the IEEE/CVF Conference on Computer Vision and Pattern Recognition*, pages 10938–10947, 2021. 3, 4, 6

[37] Yansong Tang, Zanlin Ni, Jiahuan Zhou, Danyang Zhang, Jiwen Lu, Ying Wu, and Jie Zhou. Uncertainty-aware score distribution learning for action quality assessment. In *Proceedings of the IEEE/CVF Conference on Computer Vision and Pattern Recognition*, pages 9839–9848, 2020. 1, 2, 6

[38] Du Tran, Lubomir Bourdev, Rob Fergus, Lorenzo Torresani, and Manohar Paluri. Learning spatiotemporal features with 3d convolutional networks. In *Proceedings of the IEEE international conference on computer vision*, pages 4489–4497, 2015. 2, 6

[39] Ashish Vaswani, Noam Shazeer, Niki Parmar, Jakob Uszkoreit, Llion Jones, Aidan N Gomez, Łukasz Kaiser, and Illia Polosukhin. Attention is all you need. In *Advances in neural information processing systems*, pages 5998–6008, 2017. 2, 3, 4, 6

[40] Shunli Wang, Dingkang Yang, Peng Zhai, Chixiao Chen, and Lihua Zhang. Tsa-net: Tube self-attention network for action quality assessment. In *Proceedings of the 29th ACM International Conference on Multimedia*, pages 4902–4910, 2021. 2

[41] Tianyu Wang, Yijie Wang, and Mian Li. Towards accurate and interpretable surgical skill assessment: A video-based method incorporating recognized surgical gestures and skill levels. In *International Conference on Medical Image Computing and Computer-Assisted Intervention*, pages 668–678. Springer, 2020. 1

[42] Haixu Wu, Jiehui Xu, Jianmin Wang, and Mingsheng Long. Autoformer: Decomposition transformers with auto-correlation for long-term series forecasting. *arXiv preprint arXiv:2106.13008*, 2021. 3

[43] Chengming Xu, Yanwei Fu, Bing Zhang, Zitian Chen, Yu-Gang Jiang, and Xiangyang Xue. Learning to score figure skating sport videos. *IEEE transactions on circuits and systems for video technology*, 30(12):4578–4590, 2019. 1, 2, 3, 5, 6

[44] Xumin Yu, Yongming Rao, Wenliang Zhao, Jiwen Lu, and Jie Zhou. Group-aware contrastive regression for action quality assessment. In *Proceedings of the IEEE/CVF International Conference on Computer Vision*, pages 7919–7928, 2021. 1, 2, 6

[45] Ling-An Zeng, Fa-Ting Hong, Wei-Shi Zheng, Qi-Zhi Yu, Wei Zeng, Yao-Wei Wang, and Jian-Huang Lai. Hybrid dynamic-static context-aware attention network for action assessment in long videos. In *Proceedings of the 28th ACM International Conference on Multimedia*, pages 2526–2534, 2020. 1, 2, 3, 5, 6

[46] Chuhan Zhang, Ankush Gupta, and Andrew Zisserman. Temporal query networks for fine-grained video understanding. In *Proceedings of the IEEE/CVF Conference on Computer Vision and Pattern Recognition*, pages 4486–4496, 2021. 3, 6

[47] Haoyi Zhou, Shanghang Zhang, Jieqi Peng, Shuai Zhang, Jianxin Li, Hui Xiong, and Wancai Zhang. Informer: Beyond efficient transformer for long sequence time-series forecasting. In *Proceedings of AAAI*, 2021. 3

[48] Jiaming Zhou, Kun-Yu Lin, Haoxin Li, and Wei-Shi Zheng. Graph-based high-order relation modeling for long-term action recognition. In *Proceedings of the IEEE/CVF Conference on Computer Vision and Pattern Recognition*, pages 8984–8993, 2021. 3, 6